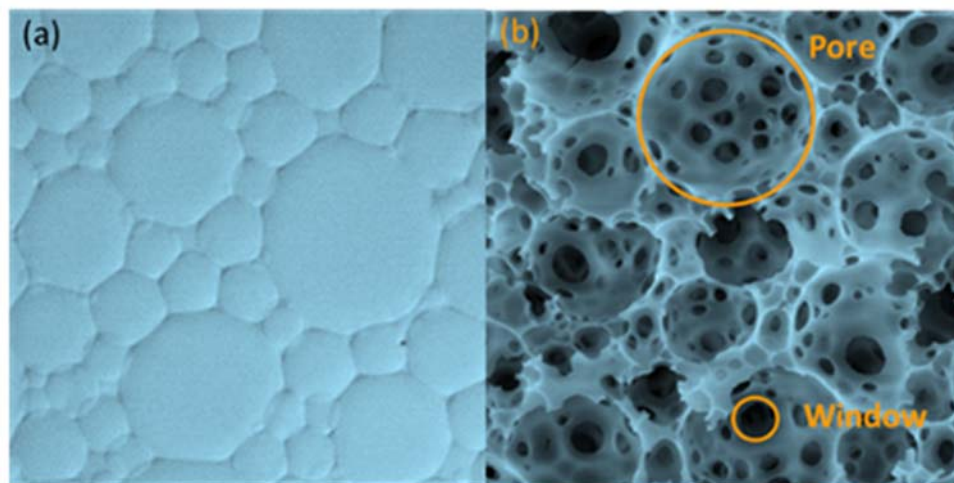


October 2016

Arsenic Removal from Water by Porous Polymers

WRRI Technical Completion Report No. 374

Reza Foudazi
Ryan Zowada
Anna Malakian



Typical images of a polyHIPE Polymer. a) Optical microscope image before polymerization. b) Scanning electron image after polymerization.

New Mexico Water Resources Research Institute
New Mexico State University
MSC 3167, P.O. Box 30001
Las Cruces, New Mexico 88003-0001
(575) 646-4337 email: nmwrri@nmsu.edu



ARSENIC REMOVAL FROM WATER BY POROUS POLYMERS

By

Reza Foudazi, Assistant Professor

Ryan Zowada, Research Assistant

Anna Malakian, Graduate Assistant

Department of Chemical and Materials Engineering

New Mexico State University

TECHNICAL COMPLETION REPORT

Account Number 125573

October 2016

New Mexico Water Resources Research Institute

In cooperation with the

Department of Chemical and Materials Engineering

New Mexico State University

The research on which this report is based was financed in part by the U.S. Department of the Interior, Geological Survey, through the New Mexico Water Resources Research Institute.

DISCLAIMER

The purpose of the New Mexico Water Resources Research Institute (NM WRRI) technical reports is to provide a timely outlet for research results obtained on projects supported in whole or in part by the institute. Through these reports the NM WRRI promotes the free exchange of information and ideas and hopes to stimulate thoughtful discussions and actions that may lead to resolution of water problems. The NM WRRI, through peer review of draft reports, attempts to substantiate the accuracy of information contained within its reports, but the views expressed are those of the authors and do not necessarily reflect those of the NM WRRI or its reviewers. Contents of this publication do not necessarily reflect the views and policies of the Department of the Interior, nor does the mention of trade names or commercial products constitute their endorsement by the United States government.

Abstract

The purpose of this study is to design a polyHIPE polymer that is super sorbent with the capability of becoming functionalized for heavy metal removal from water. PolyHIPE polymers are interconnected porous polymer structures (up to 99% porosity). The monomer used in this work is acrylamide-2-methyl-1-propanesulfonic acid (AMPS), which is cross-linked with N,N'-methylene(bis)acrylamide (MBA) to produce cation exchange monoliths which can be functionalized in-situ with iron(III) oxide nanoparticles. When monoliths are functionalized with these nanoparticles, they have the capacity to filter out heavy metal cations in water.

Scanning Electron Microscopy (SEM) and Transmission Electron Microscopy (TEM) are used to characterize the polymer and nanoparticle morphology. Immersing samples in excess water show high water capacity of such porous polymers (more than 2000 wt.%) for the first time. An induced coupled plasma mass spectrometer (ICP-OES) was used to measure the arsenic removal capability of functionalized polymers from water. The results show that a super sorbent polymer monolith can be synthesized through the HIPE polymerization technique and can be functionalized for removing heavy metals such as arsenic in water.

Keywords: high internal phase emulsion, polymerization, arsenic removal, heavy metal, water contamination, porous polymer, filtration, nanoparticle.

Table of Contents

Abstract.....	iii
Table of Contents	iv
List of Figures	v
List of Tables and Equations.....	vi
Background	1
Introduction.....	1
Arsenic removal methods.....	2
PolyHIPE Background	4
Problem Statement and Objectives.....	6
Experiment.....	7
Materials	7
PolyHIPE Synthesis.....	8
Hydrated Ferric Oxide Nanoparticle (HFO NP) Synthesis	10
SEM Characterization	12
Swelling Kinetics.....	13
TEM Characterization.....	13
Arsenic Removal Efficiency.....	13
Results and Discussion	14
Scanning Electron Microscopy.....	14
Water Uptake Analysis.....	18
Transmission Electron Microscope	20
Arsenic Removal	23
Conclusion.....	24
Supporting Information.....	25
References	27

List of Figures

Figure 1: Different emulsion systems: oil in water.....	5
Figure 2: Difference in geometries of dilute and	5
Figure 3: (a) Typical optical micrograph before polymerization, and	6
Figure 4: (a) 2-acrylamidopropanesulfonic acid, (b) N,N'-methylene	7
Figure 5: Schematic representation of polyHIPE synthesis process.....	8
Figure 6: Poly(AMPS-MBA) polymer network	9
Figure 7: Schematic illustration of HFO nanoparticles encapsulated within the polymer matrix.....	10
Figure 8: Illustration process of in situ HFO nanoparticle synthesis in a polymeric network	11
Figure 9: SEM image analysis of average pore diameter for different monomer to	14
Figure 10: SEM image analysis of average window diameter for different monomer to	15
Figure 11: Frequency of pore and window diameters. A) S_6_85 Pore diameter frequency,	15
Figure 12: Scanning electron micrographs of S_6_85 sample (monomer to cross-linker ratio of 6:1,.....	16
Figure 13: Scanning electron micrographs of S_5_85 sample (monomer to cross-linker ratio of 5:1,.....	16
Figure 14: Scanning electron micrographs of S_4_85 sample (monomer to cross-linker ratio of 4:1,.....	17
Figure 15: Scanning electron micrographs of S_5_80 sample (monomer to cross-linker ratio of 5:1,.....	17
Figure 16: Scanning electron micrographs of S_5_75 sample (monomer to cross-linker ratio of 5:1,.....	18
Figure 17: Water uptake ratio (grams of water/ grams of polyHIPE) of samples	19
Figure 18: Water uptake ratio (grams of water/ grams of polyHIPE) of samples with	20
Figure 19: TEM micrographs of S_5_85 showing HFO nanoparticles with amorphous morphology. Magnification of the images to the top left 50,000x, top right 30,000x, bottom left 20,000x, and bottom right 15,000x.	21
Figure 20: TEM micrographs of S_5_85 showing HFO nanoparticles with cubic morphology. Magnification of the images to the left is 40,000x and right 80,000x.	21
Figure 21: TEM micrographs of S_4_85 showing HFO nanoparticles with amorphous morphology.....	22
Figure 22: TEM micrographs of S_4_85 showing HFO nanoparticles with amorphous morphology.....	22
Figure 23: Percent of arsenic ions removed from solution for different porosities of functionalized	23
Figure 24: Percent of arsenic ions removed from solution for different monomer to cross-linker	24
Figure 25: Typical image analysis of SEM micrographs in MATLAB measuring window diameter	25
Figure 26: Typical image analysis of SEM micrographs in MATLAB measuring pore diameter	25

Figure 27: Concentration levels of As(V) in the water comparing different porosity 26

Figure 28: Concentration levels of As(V) in the water comparing different monomer to crosslinker..... 26

List of Tables and Equations

Equation 1: Swelling degree: variable m is the mass of the polymer after swelling, and m_0 is the initial mass..... 18

Table 1: Sizes of HFO nanoparticles within polyHIPE samples obtained from the TEM image analysis.....22

Background

Introduction

On July 28, 2010, through Resolution 64/292, the United Nations General Assembly explicitly recognized the human right to clean water and sanitation and acknowledged that clean drinking water and sanitation are essential to the realization of all human rights (UN News Center 2002). Rural and other communities may face challenges in finding water management solutions due to costs associated with the operation and maintenance of a water treatment facilities. Heavy metal contamination is one of these challenges that are caused by the rapid development of industries such as metal-plating facilities, mining operations, fertilizer manufacturing, etc. (Fu and Wang, 2011). Despite the current regulations established by the U.S. Environmental Protection Agency (EPA) and the World Health Organization (WHO), heavy metal contamination in the environment is still a major public health concern worldwide. Unlike organic contaminants, heavy metals are not biodegradable and accumulate in living organisms. Heavy metal contamination does not only occur in impoverished nations, according to EPA reports, the presence of some of these heavy metals, particularly arsenic, has also been confirmed in some brackish groundwater sources including the groundwater in New Mexico (US EPA).

Water contaminated by arsenic is found to have adverse effects on the human body when ingested (Lata and Samadder, 2016). For example, Lim and Aris (2013) reported that arsenic pollution in the West Bengal districts of India has affected many people living within that area. Inorganic arsenic is always considered a potent human carcinogen and is associated with increased risk of skin, lung, urinary bladder, liver, and kidney cancers (Choong et al., 2007).

The most common inorganic species of arsenic are As(III) and As(V), which are also known as arsenite and arsenate, respectively. As(V) is about 60 times less toxic than As(III) (Habuda-Stanić and Nujić, 2015). The less common forms of natural arsenic compounds are dimethylarsinate (or DMA) and monomethylarsonate (or MMA), known as organic arsenic. The toxicity of different arsenic species varies in this order: As(III) > As(V) > MMA > DMA. The focus of this preliminary study on porous polymer for heavy metal removal is As(V).

In addition to the detrimental health effects, heavy metal contamination can interfere with some of the most common water treatment methods such as nanofiltration (NF) and reverse osmosis (RO). Heavy metals can cause membrane fouling for NF and RO systems causing significant concerns

in advanced water treatment (Kim et al. 2011). Therefore, sequestration of heavy metals as pretreatment for membrane filtration can significantly improve their efficiency and membrane lifetime. Most common forms of removal involve conversion into different compounds and then aggregation for filtration, or transformation into insoluble compounds in combination with other elements, such as iron (Choong et al., 2007).

This purpose of this study is to determine if a new method of arsenic removal is possible using super sorbent highly porous polymer monoliths, synthesized by polyHIPE templating, can be functionalized by in situ synthesis of hydrated ferric oxide nanoparticles. The composite system will be tested to see if the particles have a coulombic interaction with the arsenic ions, and adsorb them to the surface of the polymer when contaminated water passes through the polymer monolith. This system will have advantages over the current coagulation and filtration methods due to removing the need to filtrate aggregates and having a higher permeability than NF and RO membranes increasing the rate of process.

Arsenic removal methods

Due to the adverse health effects of heavy metals, developing solutions for their removal has received considerable research attention. Heavy metals have been treated by different methods such as membrane separation, chemical precipitation, coagulation and flocculation, ion-exchange (or chelation), and adsorption (Jadhav et al., 2015). Among these methods, adsorption offers several advantages including simple operation, easy handling of waste, absence of added reagents, compact facilities, easy scalability, and generally low operating costs (Habuda-Stanić and Nujić, 2015).

In 2011, As(V) removal was achieved effectively by an ion exchange method, with less than one milligram per liter of arsenic in the effluent, while As(III) was not eliminated, and a prior oxidation step was required (Litter et al. 2010). Arsenite, As(III), was not removed most likely because it does not have a charge at a pH of 7, unlike As(V) which is susceptible to ion exchange. Arsenite and arsenate both have four different valence species. The four As(III) species are: H_3AsO_3 , H_2AsO_3^- , HAsO_3^{2-} , and AsO_3^{3-} that exist at pH of <less than 9.22, 9.22, 12.13, and 13.4, respectively. The As(V) species are: H_3AsO_4 , H_2AsO_4^- , HAsO_4^{2-} , and AsO_4^{3-} that occur at pH of < 2.2, 2.2, 6.97, and 11.53, respectively (Fendorf et al. 2010). Due to arsenite having a neutral charge there is usually an oxidation step required before its removal.

Membrane technologies, especially RO and NF, can be used for arsenic removal (Jadhav et al., 2015). However, as mentioned before, arsenic can increase membrane fouling (Choonget al. 2007). Höll (2010) showed that nanofiltration, which usually shows removal of divalent species, can eliminate As(III) and As(V) species predominantly through size exclusion. Arsenic removal rates in bench and pilot-scale experiments ranged from 60% - 90%. Höll (2010) also found that RO in both lab and pilot-scale experiments could effectively remove more than 95% As(V) and 74% As(III). These membrane technologies, however, have low permeability causing the process to be time consuming and costly.

Adsorption is a promising method since it does not produce undesirable by-products, and can be regenerated for reuse for a number of cycles (Lata and Samadder, 2016). Various materials have been used as adsorbents such as surfactants (Lata and Samadder, 2016), synthetic activated carbon, industrial byproducts and wastes (Ghorbani, Eisazadeh, 2013), ferrous material, iron-based soil amendment, and mineral products. However, most arsenic adsorption technologies use innocuous hydrated metal oxides (HMOs) with high arsenic affinity (Padungthon et al. 2015). Biosorption is a method of adsorption that has received a lot of attention because of its advantages with using natural abundant materials, nontoxicity, environment friendliness and cost effectiveness (Dambies, 2005). Biocomposites such as alginate (Hassan et al. 2014), microalgae, chitin, and chitosan (Boddu et al. 2008) have also been studied for the removal of heavy metals due to their biodegradability and eco-friendliness. However, bioadsorbents have poor chemical and mechanical resistance (Zhao et al., 2011) compared to polymeric adsorbents already in the market. Nano-adsorption can be used for arsenic removal using nanoparticle's unique properties, such as catalytic potential, large surface area, high reactivity, easy separation, and large number of active sites (Lata and Samadder, 2016). The development of nano-adsorbents for arsenic removal has explored various transition metal-based compounds such as copper, iron, and titanium. Usually, adsorption on nano-adsorbents has three steps: first the adsorbate molecule is transported to the adsorbent surface by diffusion through the boundary layer; second the adsorbate diffuses from the external surface into the pores of the adsorbent; and third the adsorbate binds on the active sites of the internal pores (Höll, 2010).

In recent years nano-sized iron oxides have attracted growing interest in water treatment and environmental remediation. An et al. (2011) showed nearly complete arsenic removal by employing a new method of starch-bridged magnetite nanoparticles. However, the small size of

nanoparticles induces issues involving mass transport and excessive pressure drops when applied in a fixed bed or any other flowing systems. Therefore, certain difficulties arise in separation and reuse, and there is even a possible risk to ecosystems and human health with nanoparticles (Lofrano et al., 2016). Coagulation can also remove up to 99 % of the arsenic (Choong et al. 2007). Arsenic can be removed most commonly by precipitation as ferric arsenate, calcium arsenate, or arsenic sulfide (Jadhav et al., 2015). Even though there is a high removal rate with coagulation, the process must be allowed time for settlement of coagulates in the water, and then removal through filtration. An effective approach to overcoming the issues related to nano-adsorbents is to use a host for the nanoparticles. Polymeric hosts are an attractive choice because of their controllable pore size (Lofrano et al., 2016) and surface chemistry. This is a promising class of adsorbent materials for heavy metal contamination removal. In this study, a polymeric host for incorporation of hydrated ferric oxide (HFO) nanoparticles is used. The polymeric host is created through high internal phase emulsion (HIPE) templating to maximize the surface area and allow tuning of the pore size and permeability. The polyHIPE is an economical choice in the fact that only 5 – 20% of the volume is polymer. This polymeric host method would be an advantage over coagulation by combining the arsenic removal and water filtration process simultaneously. The polyHIPE can also be formed to a custom shape by placing it into a mold before polymerization. This gives the method several options for removal methods that is packed bed column, beads, monolith, etc.

PolyHIPE Background

The polymeric host chosen for this study is a high internal phase emulsion (HIPE) templated polymer, also known as PolyHIPE. PolyHIPEs are polymers with high porosity (can reach over 90%) with interconnected pores and windows. Therefore, polyHIPEs can have a fast water uptake due to the capillary effect when immersed in water.

Emulsions are the dispersion of liquid droplets (internal phase) into another immiscible liquid (external phase). These two liquids are generally considered to be an oil and water phase that are thermodynamically stabilized with a surfactant (or emulsifier). The surfactant stabilizes the system by adsorption at the surface of droplets lowering the interfacial tension between water and oil phases. The surfactant is only soluble in one of the phases to ensure it encapsulates the internal phase droplets preventing a possible phase inversion. Two basic types of emulsions are water-in-oil (W/O) and oil-in-water (O/W) (Figure 1). When the dispersed phase of an emulsion is greater

than 74% of the total volume it is considered a high internal phase emulsion (HIPE). This percentage is considered the maximum close packing of monodispersed spheres for face center cubic unit cells (Cameron, 2005). Once the volume percent exceeds this threshold the spheres begin to deform into polyhedron shapes (Figure 2). This deformation will create large areas of contact between droplets, and a packed configuration that induces mechanical interference between droplets, thus, prohibiting their free movement (Lissant, 1966).

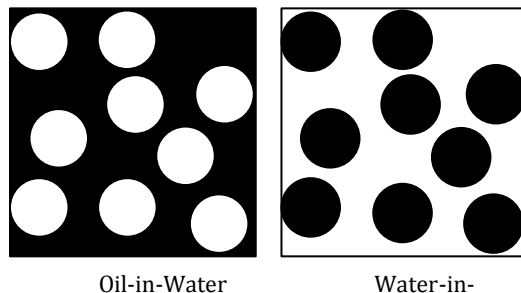


Figure 1: Different emulsion systems: oil in water (O/W) and water in oil (W/O)

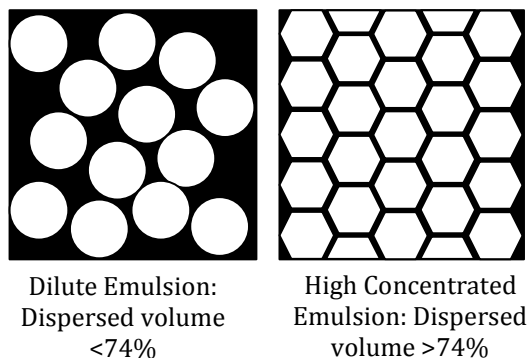


Figure 2: Difference in geometries of dilute and highly concentrated emulsions

Emulsions can be polymerized by three methods: polymerization of both phases (continuous and dispersed phases) to produce composites; polymerization of the dispersed phase to produce colloidal particles; or polymerization of the continuous phase and removing the dispersed phase to produce porous materials (Zhang and Cooper, 2005). To polymerize a HIPE, the continuous phase should contain monomers and may contain a cross-linker, which binds the polymer chains to form a network structure enhancing the mechanical properties of final monolith. Following polymerization of the continuous phase, the emulsion droplets are embedded in the resulting material. Under the correct conditions (*vide infra*), small interconnecting windows form between

adjacent emulsion droplets upon polymerization allowing the dispersed phase to be removed by drying and creating voids (where droplets were before) in polyHIPEs. Therefore, a highly porous and permeable material with complex pore morphology is produced (Figure 3).

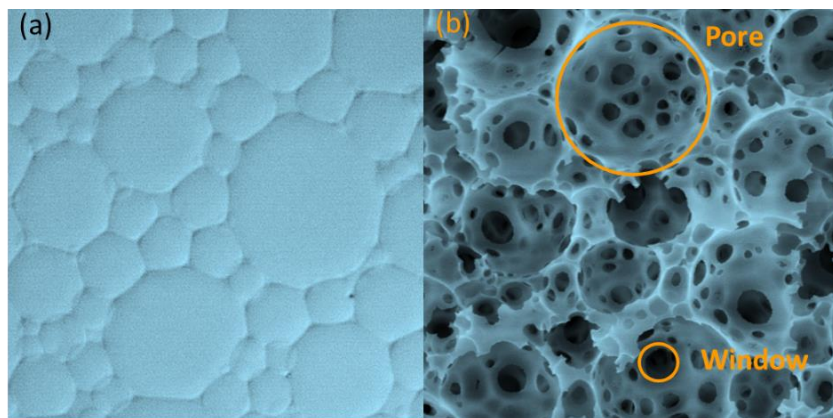


Figure 3: (a) Typical optical micrograph before polymerization, and (b) scanning electron micrograph after polymerization, of a polyHIPE.

PolyHIPEs are further classified by their size and shape. PolyHIPEs can be synthesized as beads through a water-in-oil-in-water (W/O/W) or an oil-in-water-in-oil (O/W/O) emulsion templating methods, polymerized as a thin membrane, or polymerized as a bulk material also known as a monolith. This report will focus on monolith polyHIPEs as a mean for a polymeric host for water remediation, particularly arsenic removal, for the first time.

Problem Statement and Objectives

The main concern of this work is to remove arsenic contamination from water resources in order to provide economical strategies for drinking water in New Mexico. The initial standard for arsenic contamination in drinking water was 0.05 mg/L, or 50 ppb, established in 1942 by the Public Health Service. The Environmental Protection Agency (EPA) has regulated the arsenic maximum contaminant level (MCL) to 10 ppb in 2006. Several regions in New Mexico have high probability of occurrence of arsenic above the MCL of 10 ppb, with high expected individual risk for arsenic exposure from ground water. Arsenic contamination can be removed from water resources through adsorption, ion exchange, coagulation/ filtration, oxidation/ filtration, nanofiltration, and reverse osmosis (RO). While the latter is expensive compared to most other methods, it is widely used to

bring the water quality into compliance with the EPA requirement. Adsorption methods are less expensive and can be adapted to rural areas and small communities.

The specific objectives of this project are: (i) studying the emulsion formation and polymerization of 2-acrylamidopropanesulfonic acid (AMPS), (ii) investigating the generation of hydrated iron(III) oxide nanoparticles on the polymer chains, and (iii) exploring the adsorption/desorption of arsenic on/from synthesized porous polymers.

Experiment

Materials

Anhydrous iron(III) chloride (FeCl_3 , purchased from Sigma-Aldrich 97%) was used for the synthesis of iron nanoparticles. PolyHIPE monoliths were synthesized with the continuous phase containing 2-acrylamidopropanesulfonic acid (AMPS, purchased from Sigma-Aldrich, 99%) as the monomer, N,N' -methylene-*bis*-acrylamide (MBA, purchased from Sigma-Aldrich, 99%) as the cross-linker, Pluronic F68 (provided by BASF) as a surfactant, and potassium persulfate (KPS, purchased from Arcos-Organics, 99+%) as the thermal initiator (Figure 4). The dispersed phase of polyHIPEs was produced with cyclohexane (purchased from Pharmco-Aaper, >99%). The arsenic stock solution was prepared by using arsenic pentoxide (purchased from Spectrum).

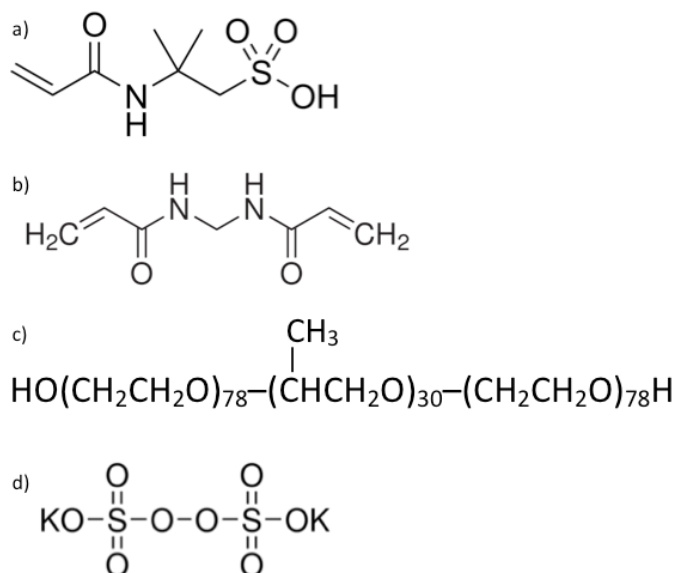


Figure 4: (a) 2-acrylamidopropanesulfonic acid, (b) N,N' -methylene-*bis*-acrylamide, (c) Pluronic F68, and (d) potassium persulfate

PolyHIPE Synthesis

HIPEs were prepared on a 40-gram basis (this was chosen to ease the mechanical mixing) with an overhead mixer (Talboys Model 4136 Stirrer, manufactured by Henry Troemner, LLC). The aqueous (water) phase was comprised of 55 wt.% water to ensure there is enough water to dissolve the other components of the aqueous phase. The surfactant, Pluronic F68, was 20 wt.% of the aqueous phase, an amount chosen to ensure stability of emulsions. The thermal initiator, potassium persulfate (KPS), was 1 wt.% of the aqueous phase. The remaining 24 wt.% contained water soluble monomer and cross-linker, which were AMPS and MBA, respectively. The concentration of AMPS to MBA was varied in 6:1, 5:1, and 4:1 weight ratios. These ratios were established to find the optimal cross-link density for polyHIPEs to ensure good mechanical strength and swelling capability. The aqueous phase solution was mixed with the overhead mixer at 250 RPM until complete dissolving occurred.

Cyclohexane, as dispersed phase, was added drop-wise by using a syringe and an automated syringe pump (KD Scientific 120 Push/Pull Syringe Pump) under a fume hood. The mixing speed was 350 RPM initially and increased to 450 RPM incrementally (increased every ten mL of cyclohexane dispersed) to ensure good mixing as the viscosity of the emulsions increased (Figure 5). To ensure the correct volume of cyclohexane was added (as cyclohexane may evaporate during emulsification), emulsions were weighed before and after the cyclohexane was added.

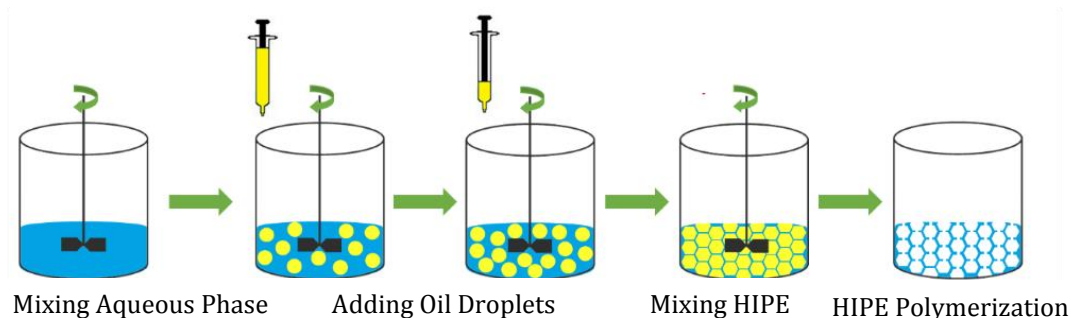


Figure 5: Schematic representation of polyHIPE synthesis process

After the dispersion of oil phase and without additional mixing, the HIPEs were transferred into glass vials. The glass vials were then moved into an oven for polymerization at 65°C under ambient pressure for 24 hours. During the polymerization the AMPS monomer was cross-linked with the MBA to create a complex polymer network (Figure 6). After polymerization, the samples were

removed from the vials and heated to remove the cyclohexane and dried at 50°C in a vacuum oven. Once the oil phase, cyclohexane, had been removed, a porous polyHIPE monolith remained.

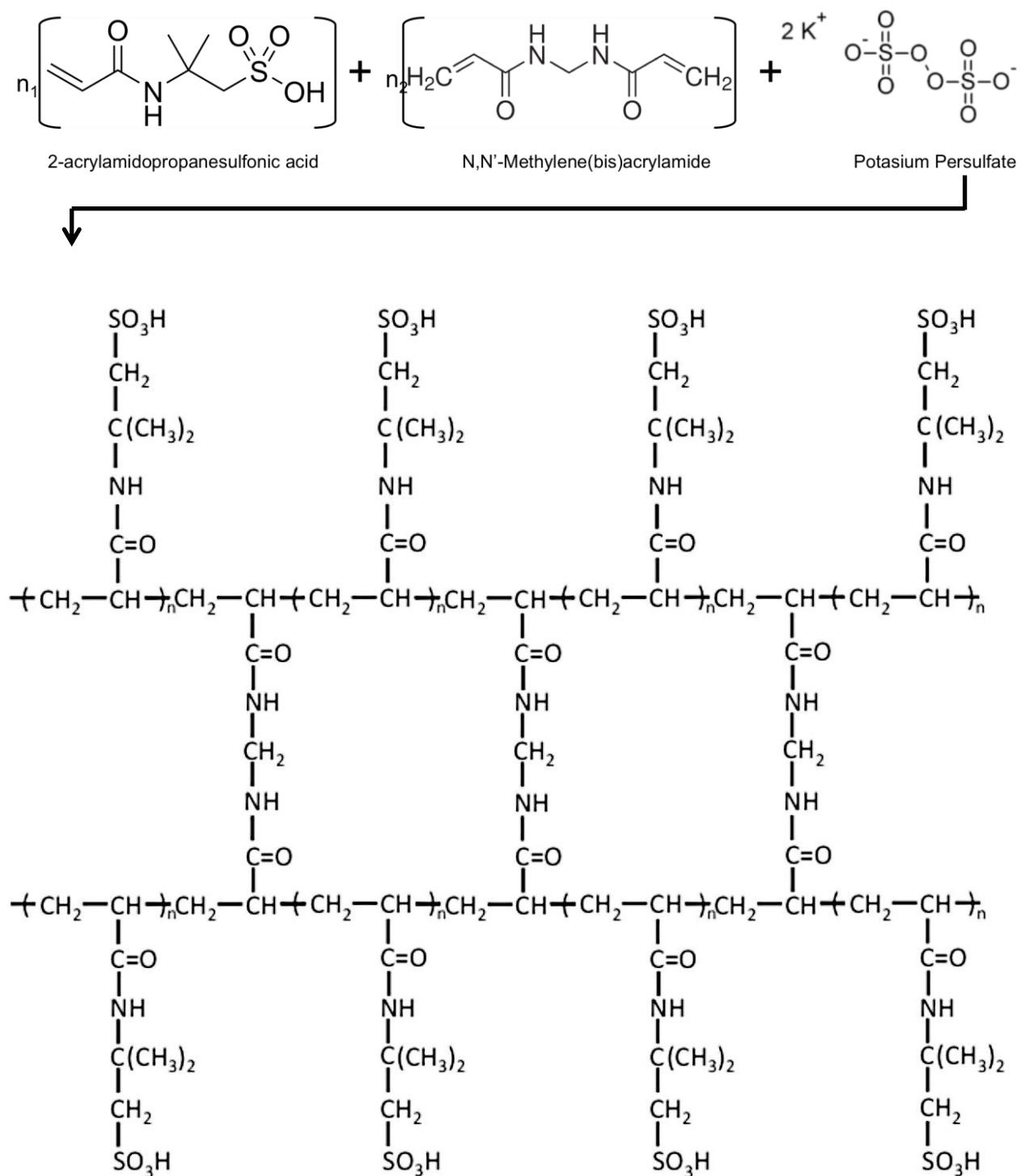


Figure 6: Poly(AMPS-MBA) polymer network

Several samples were prepared to find a proper operating window for HIPE preparation and polymerization in this work. Then, five different samples were studied varying the weight ratio of AMPS to MBA (6 to 1, 5 to 1 and 4 to 1) and varying the volume fraction (75, 80 and 85%) of oil phase, thus, controlling the porosity. The samples were named first by their monomer to cross-linker ratio then by their porosity percentage, for example a sample with a 5 to 1 weight ratio of monomer to cross-linker and 85% porosity would be named “S_5_85”. When varying the monomer to cross-linker ratio the porosity was kept constant at 85%, and while varying the porosity the monomer to cross-linker ratio was kept constant at 5 to 1.

Hydrated Ferric Oxide Nanoparticle (HFO NP) Synthesis

The in-situ synthesis of the hydrated ferric oxide nanoparticles (HFO-NPs) in the polymeric host can be performed for heavy metal removal applications (Cumbal and Sengupta 2005). This reaction irreversibly encapsulates the HFO-NP in the polymer matrix (Figure 7). The arsenic ions are adsorbed through a coulombic interaction with the embedded HFO-NPs. The arsenic can then be desorbed using a sodium hydroxide solution to regenerate the adsorbent.

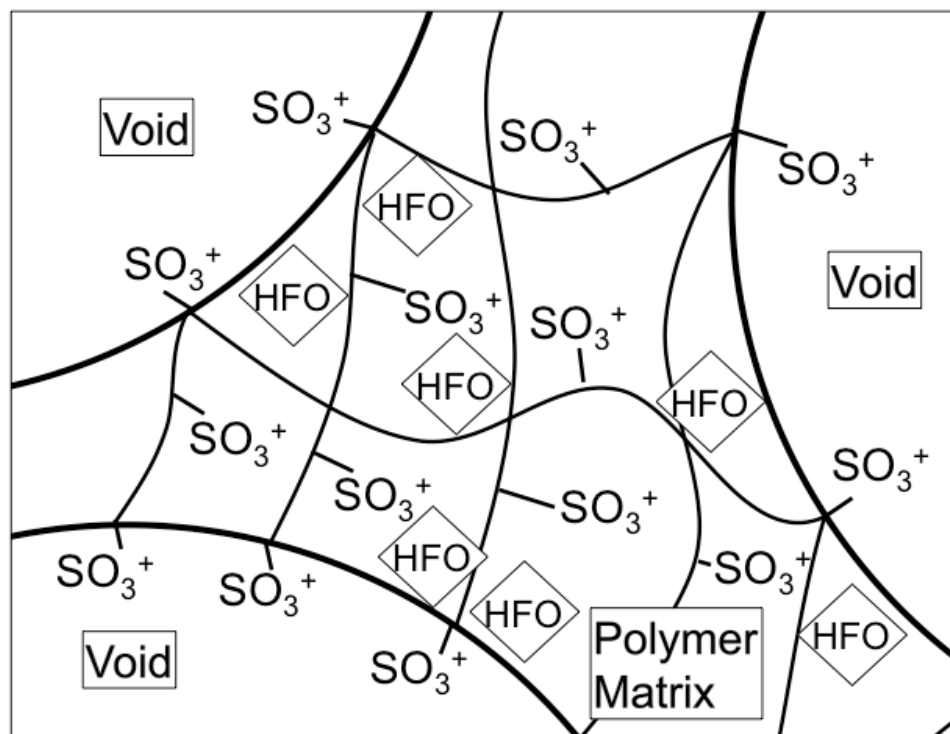


Figure 7: Schematic illustration of HFO nanoparticles encapsulated within the polymer matrix

The procedure for the in-situ synthesis of HFO particles in polyHIPE is illustrated in Figure 8. At first, small sections (approximately 0.1 gram per sample) was taken from each sample. Next a ferric chloride solution (4 wt.%) was prepared by dissolving anhydrous ferric chloride (FeCl_3) in deionized water. The polyHIPE sections were immersed in an excess amount of ferric chloride solution. The iron cations in the solution attach to the sulfonic acid groups on the polymerized AMPS. The pH of the solution was monitored throughout the immersion to ensure it was equal to or less than two to prevent oxidation of the iron cations before attaching. The samples remained immersed in the solution for 24 hours, while refreshing the solution every several hours to ensure maximum loading.

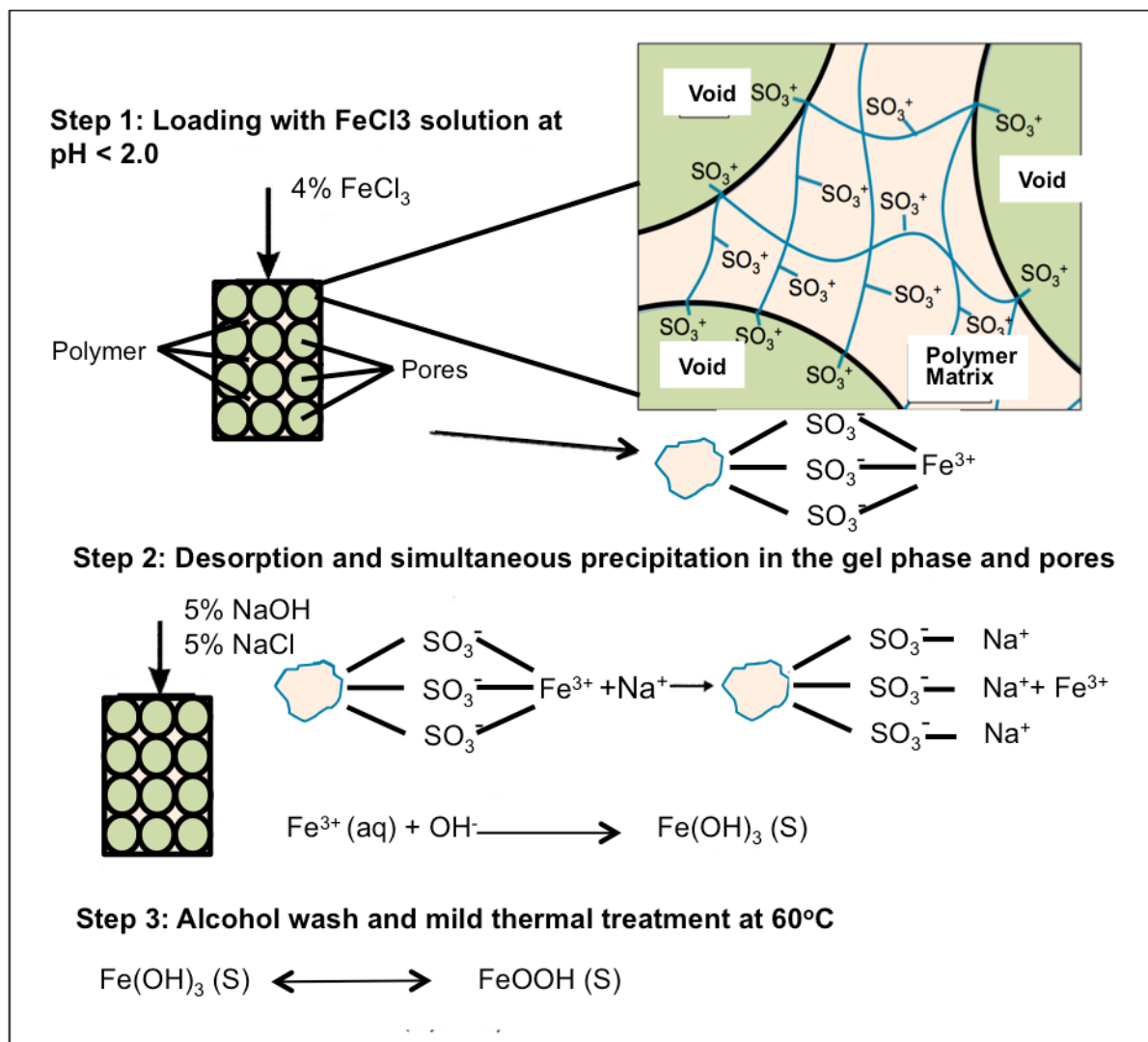


Figure 8: Illustration process of in situ HFO nanoparticle synthesis in a polymeric network

The samples were then immersed in NaOH and NaCl at 5% w/v concentrations, and soaked until they reached equilibrium. This process detaches the iron cations from the sulfonic acid groups, and replaces them with the sodium cations. The samples immediately changed color, an indication of the reaction, from an orange color in several seconds to a dark rust color after several minutes. Fresh solution of NaOH/NaCl was replenished 3 to 5 times to ensure all the iron cations were detached from the sulfonic acid groups.

In the next step, samples were washed with a solution of 50/50 (v/v) ethanol-water to ensure the HFO nanoparticles (amorphous and crystalline) were physically loaded into the polymer matrix. Consequently, the aqueous iron cations would agglomerate into solid $\text{Fe}(\text{OH})_3$ nanoparticles within the polymer matrix. The solution was removed and replaced with fresh washing solution every four to eight hours for the completion of sodium and chloride removal. To ensure the samples had been properly washed, their ionic conductivity was measured with a Hach HQ40d portable pH and ion conductivity meter. The samples were removed from the ethanol-water solution soaked in deionized water for several minutes before measuring the ion conductivity. When the samples no longer showed a change in ion conductivity between washings it was assumed the sodium chloride ions were removed. The particles synthesized have two distinct morphologies: amorphous and cubic. The cubic morphology occurs when a large amount of amorphous particles combine. The agglomeration of the nanoparticles is dependent on the local concentration of water to ethanol, where the higher the water concentration, the more the particles will agglomerate (Ramimoghadam et al. 2014).

The final step was to put samples into a convection oven for one hour at 60°C as a mild thermal treatment. This allowed the agglomeration of the solid $\text{Fe}(\text{OH})_3$ nanoparticles to crystallize and become FeOOH or HFO nanoparticles. The samples were then characterized to confirm that the nanoparticles had been embedded.

SEM Characterization

The morphology and pore and window sizes of samples were characterized under a scanning electron microscope (SEM). The morphologies of polyHIPE monoliths without hydrated ferric oxide nanoparticles were studied. Small sections of the polyHIPE samples were removed, and dried for an additional 24 hours to ensure all moisture was removed. The samples then were sputter coated with a gold filament for two minutes under argon gas to make the surface conductive. The

samples were then characterized by the S-3400N II Scanning electron microscope from Hitachi High-Technologies Corp.

Swelling Kinetics

Small sections (~0.01g) of dried polyHIPE polymer samples were immersed in excess deionized water at ambient temperature, and allowed to swell over time. The sample was removed from the water and placed in a glass vial where the excess water could be removed by a syringe. The sample was then weighed and returned into the water to continue swelling.

TEM Characterization

The transmission electron microscope was used to characterize polyHIPE monoliths functionalized with the HFO nanoparticles. Each sample was prepared in Embed 812 resin (from Electron Microscopy Sciences) to infiltrate the pores of the sample. The sample was soaked in ethanol (99%) for six hours to assist the infiltration of the resin. The ethanol was then decanted while the resin was added. Each sample was soaked in the resin for 12 hours before being transferred into a mold with fresh resin, and finally cured for 24 hours at 60°C. After embedding step, the sample was sliced into small sections with a Leica EM UC6 ultra microtome. The samples were carved with a glass knife to get small cross sections less than 100 nm thick, which were then moved onto a copper grid. The samples were analyzed by a H-7650 Transmission Electron Microscope from Hitachi High-Technologies Corp.

Arsenic Removal Efficiency

The arsenic sorption behavior of the monoliths was studied by using batch isotherm tests. The monoliths were immersed in a solution with 4.5 milligrams of arsenic per liter (4.5 ppm) of water. The solution was prepared by dissolving 9 milligrams of arsenic pentoxide in 500 mL of DI water. The pH of the solution was kept at 7.2 (pH of drinking water) using dilute NaOH and HCl solutions. The amount of polyHIPE that was functionalized with HFO nanoparticles was 0.1 g. The functionalized polyHIPEs were soaked in the arsenic solution for 24 hours. For measuring the arsenic removal efficiency, the reduction of ions through sorption was measured by a Perkin Elmer 4300 ICP-OES through induced coupled plasma optical emission spectrometry. The As(III) ion

was not tested for two reasons: the chemical As(III) was not readily available, and previous arsenic removal studies concerning As(III) have been performed under a nitrogen atmosphere in a glove box to ensure that As(III) had not been oxidized into As(V). In other words, removal of As(V) is more critical as As(III) can be oxidized to As(V).

Results and Discussion

Scanning Electron Microscopy

The scanning electron microscope shows the polymer monoliths are very porous and interconnected (Figures 12 through 16). The range and average pore diameter and window diameter were obtained through image analysis using MATLAB (Figure 9 – 11, and Figures 25 and 26). Through image analysis, it was found that there is a direct correlation between average pore/window diameter and the monomer to cross-linker weight ratio. The average pore diameter increases with a decrease in the weight of cross-linker possibly due to a less interconnected polymer network allowing the droplets to form larger pores. The number of windows decrease significantly from the 6:1 ratio to the 4:1 ratio, which could be due to a thicker pore wall originated from a more connected polymer network. The range of window and pore sizes also decreases as the amount of cross-linker increases.

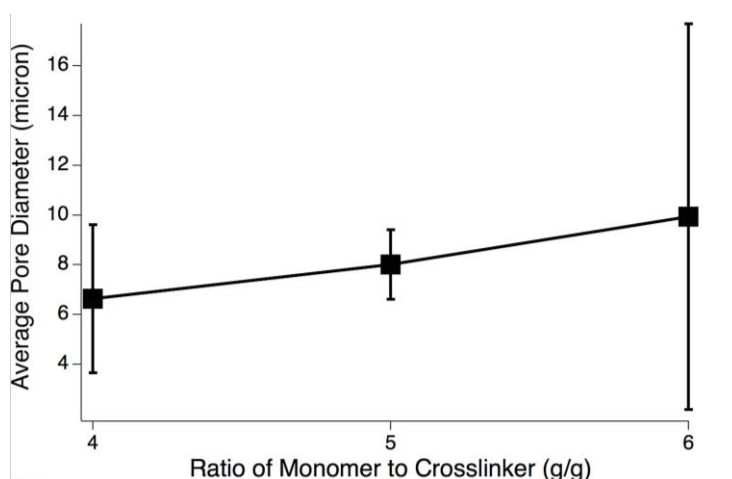


Figure 9: SEM image analysis of average pore diameter for different monomer to cross-linker ratios. The vertical lines do not show error bars but the standard deviation of droplet size distribution.

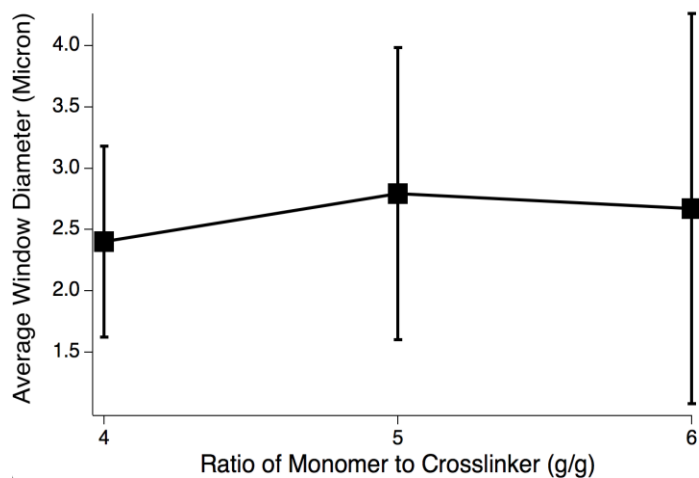


Figure 10: SEM image analysis of average window diameter for different monomer to cross-linker ratios. The vertical lines do not show error bars but the standard deviation of window size distribution

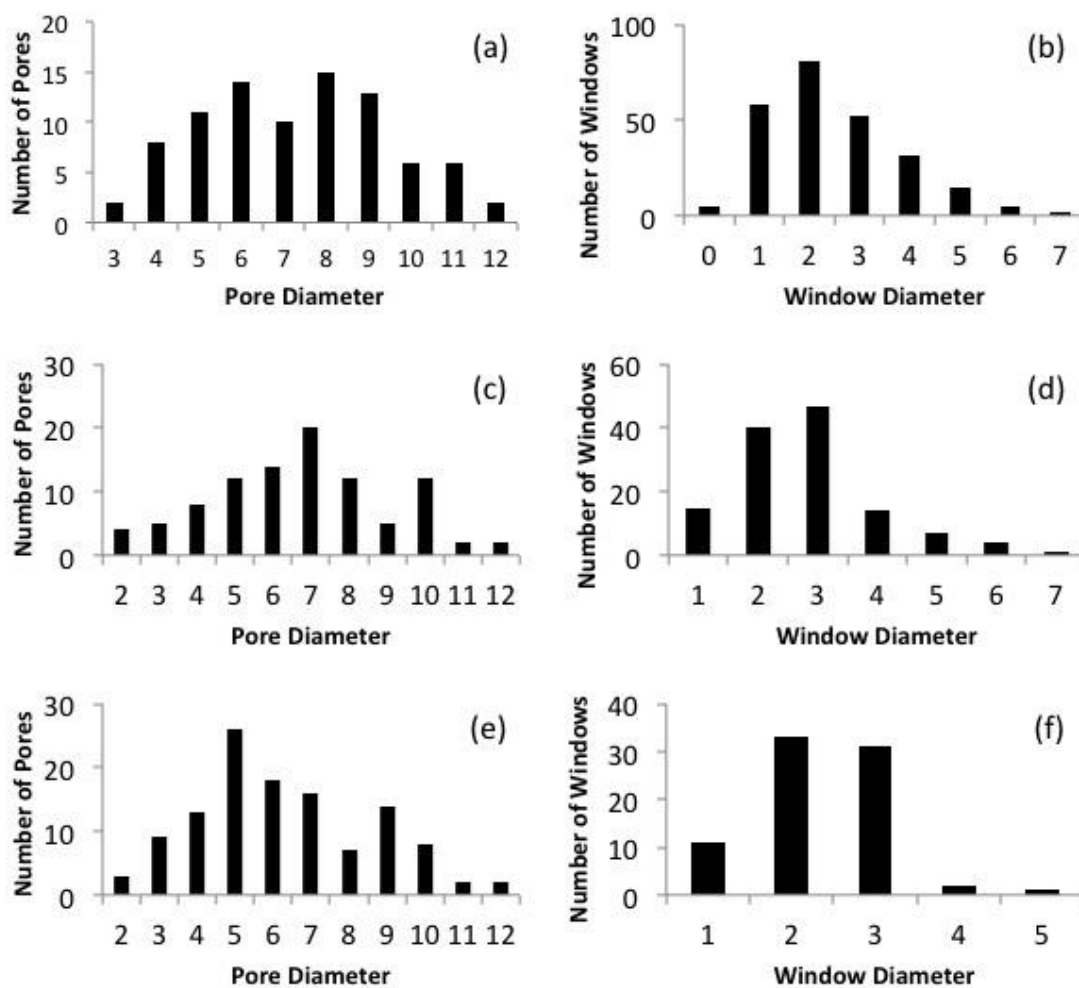


Figure 11: Frequency of pore and window diameters. A) S_6_85 Pore diameter frequency, B) S_6_85 Window diameter frequency, C) S_5_85 pore diameter frequency, D) S_5_85 window diameter frequency, E) S_4_85 pore diameter frequency, F) S_4_85 window diameter frequency.

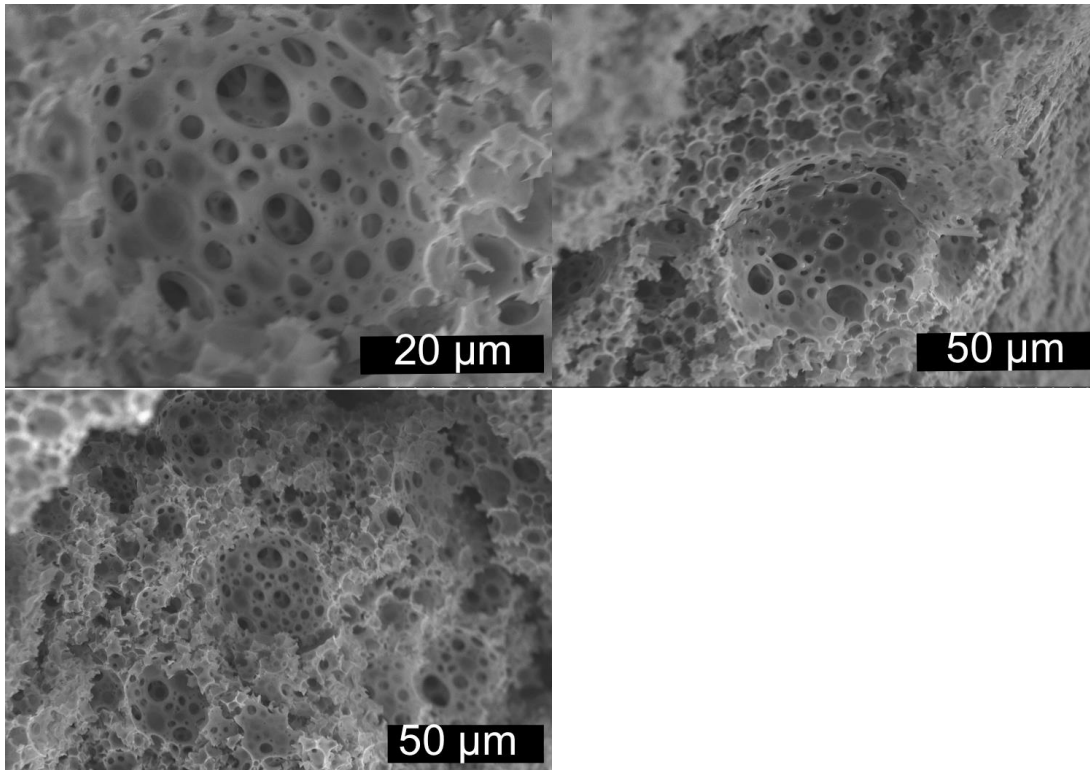


Figure 12: Scanning electron micrographs of S_6_85 sample (monomer to cross-linker ratio of 6:1, porosity of 85%) .

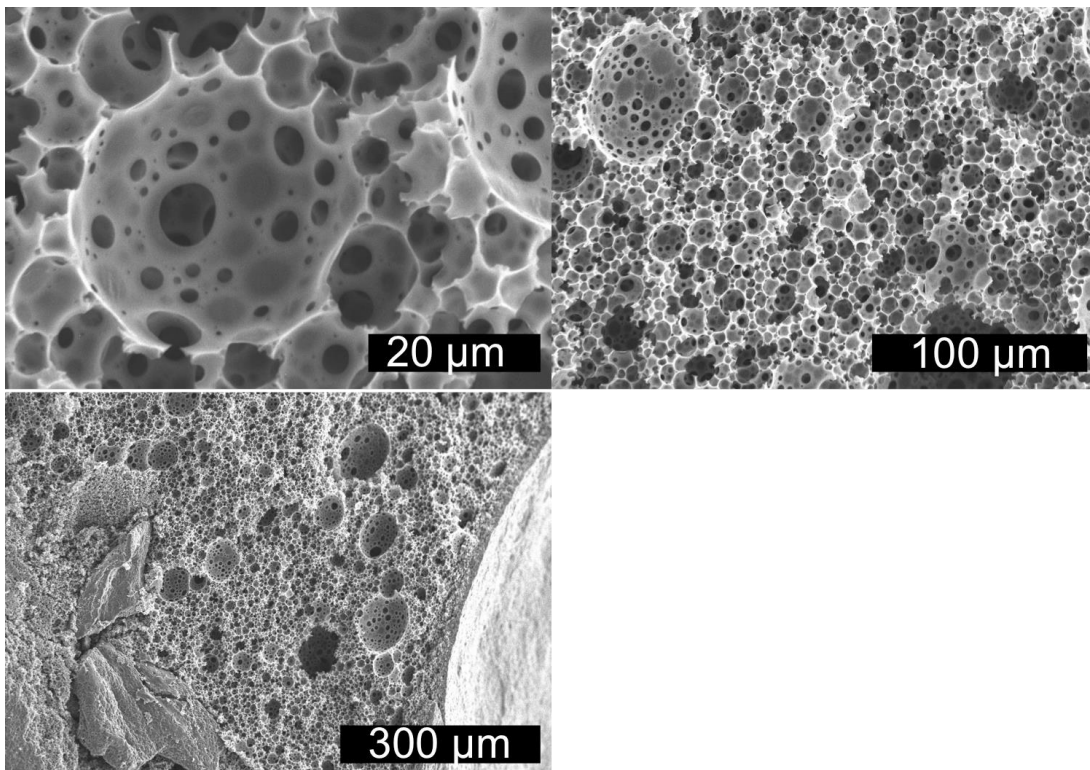


Figure 13: Scanning electron micrographs of S_5_85 sample (monomer to cross-linker ratio of 5:1, porosity of 85%)

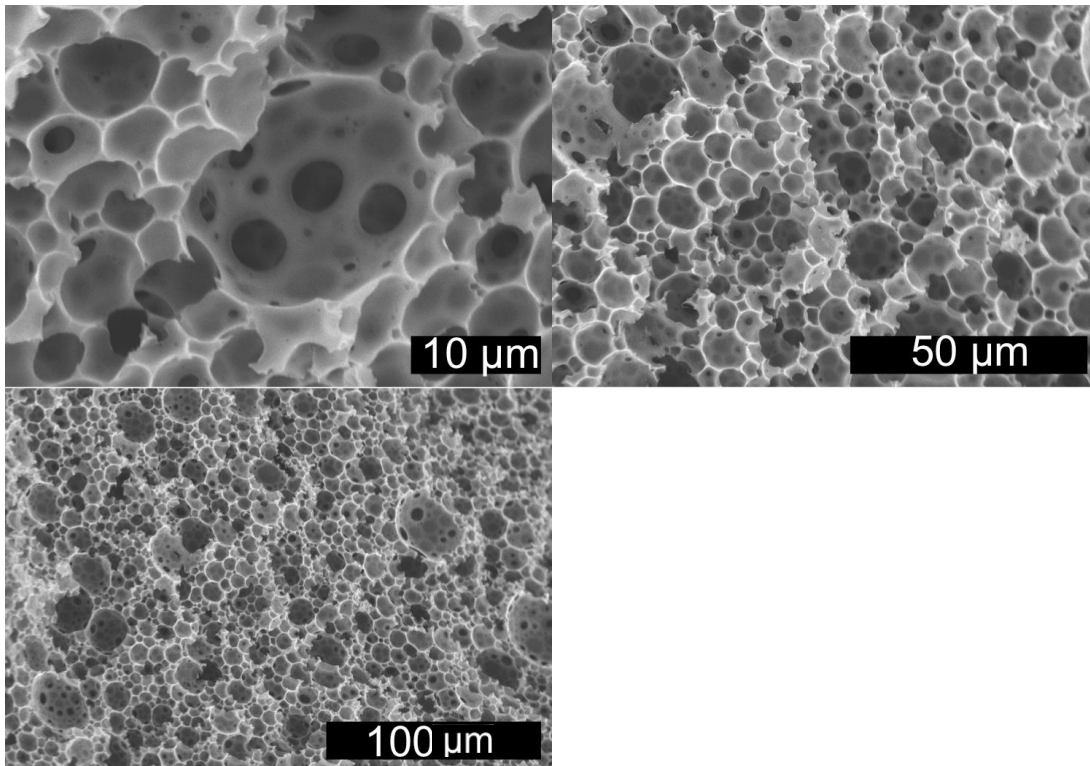


Figure 14: Scanning electron micrographs of S_4_85 sample (monomer to cross-linker ratio of 4:1, porosity of 85%)

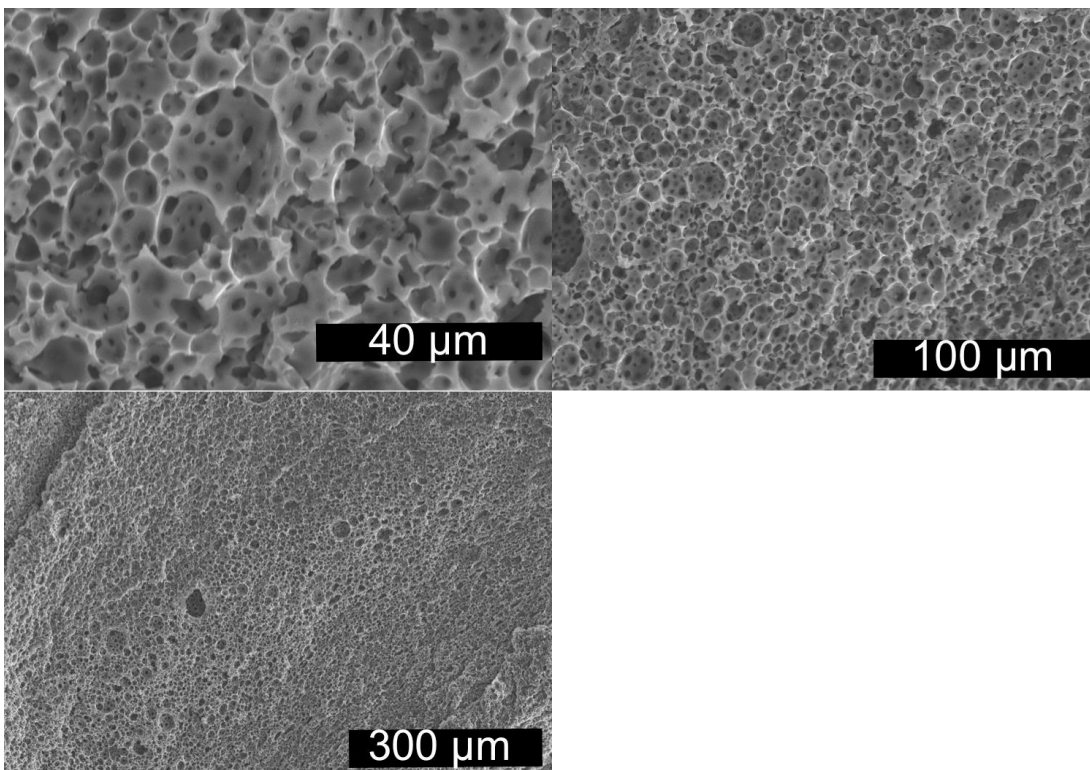


Figure 15: Scanning electron micrographs of S_5_80 sample (monomer to cross-linker ratio of 5:1, porosity of 80%)

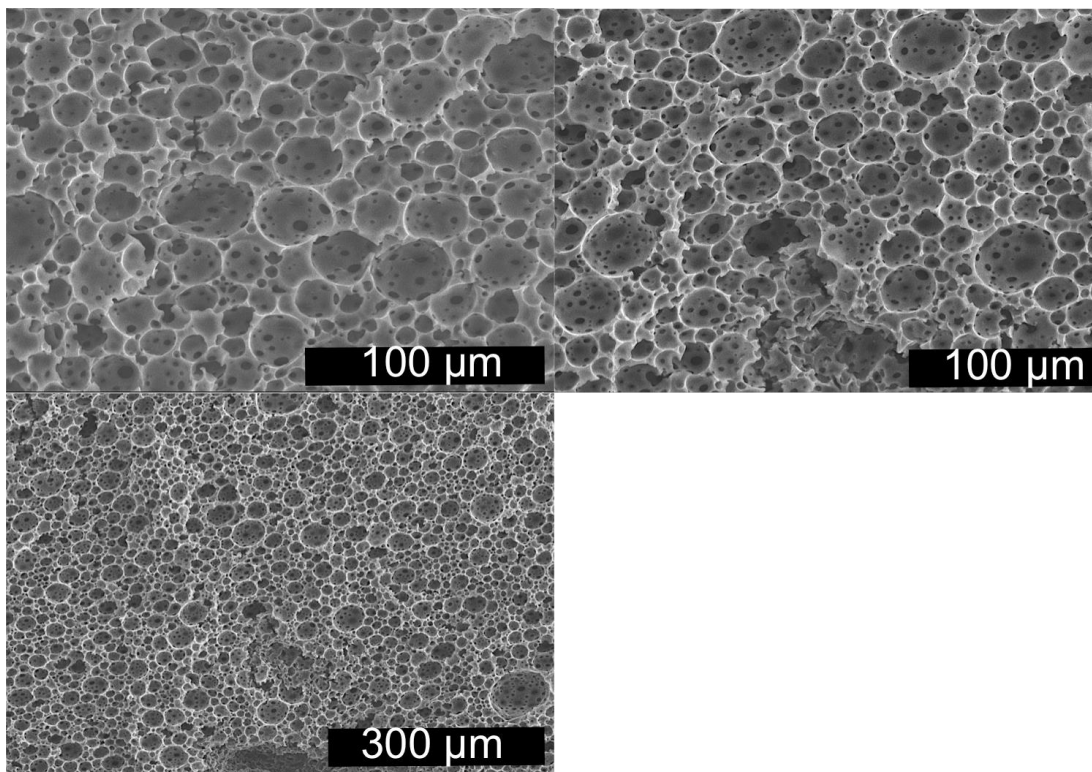


Figure 16: Scanning electron micrographs of S_5_75 sample (monomer to cross-linker ratio of 5:1, porosity of 80%)

In literature reports related to testing polymeric hosts using HFO nanoparticles, Donnan exclusion effect was an issue as it forced out the arsenic ions from the polymer (Cumbal and Sengupta 2005). This issue occurred when the pore sizes of the polymer beads were too small and the charge of the sulfonic groups prevented the arsenic ions from reaching the surface to bind to the HFO nanoparticles in the polymer matrix. To combat this issue in the current work, the polymer pore sizes are considered to be in the macroporous range, that is pore diameter are bigger than 0.5 μm .

Water Uptake Analysis

Water uptake studies showed that the samples have a hydrophilic nature, which allows them to absorb water rapidly reaching near the maximum uptake capacity in less than ten minutes. The water uptake degree can be calculated by following equation:

$$W = \frac{m}{m_0}$$

Equation 1 Swelling degree: variable m is the mass of the polymer after swelling, and m_0 is the initial mass

The water uptake of the polyHIPEs was recorded in triplicate for one hour (as a plateau was reached after 50 minute), and showed a maximum weight percentage increase of over 1500% for all samples. Such high water sorption capacity, which we call it supersorption behavior, is unique and very rare among current hydrogels, and will be developed for other water-related research by PI's research group. The maximum water uptake ratio has a direct correlation to monomer to cross-linker weight ratio. The correlation is that the more crosslinked the structure the less water uptake will occur (Figure 17). There was some correlation between the uptake degree and the porosity in such a way that the highest porosity (85%) absorbed more water than the other percentages (75 and 80%), but the sample with 75% porosity showed to absorb more water than 80% one (Figure 18). There is a possible “trade-off” with these polyHIPEs due to their hydrophilic nature. This trade off would occur between 75 and 85% porosity, where the hydrophilic nature of the polymer overtakes the water sorption contribution of capillary action from porosity. In other words, 75% sample has more hydrophilic polymer to absorb the water imparting a stronger effect on water uptake.

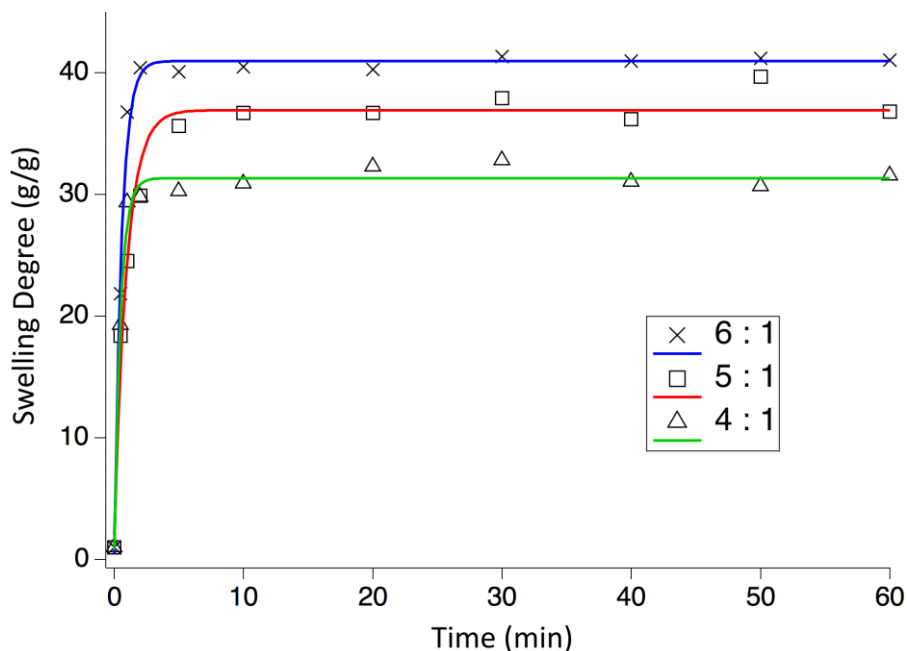


Figure 17: Water uptake ratio (grams of water/ grams of polyHIPE) of samples with different monomer to cross-linker weight ratio

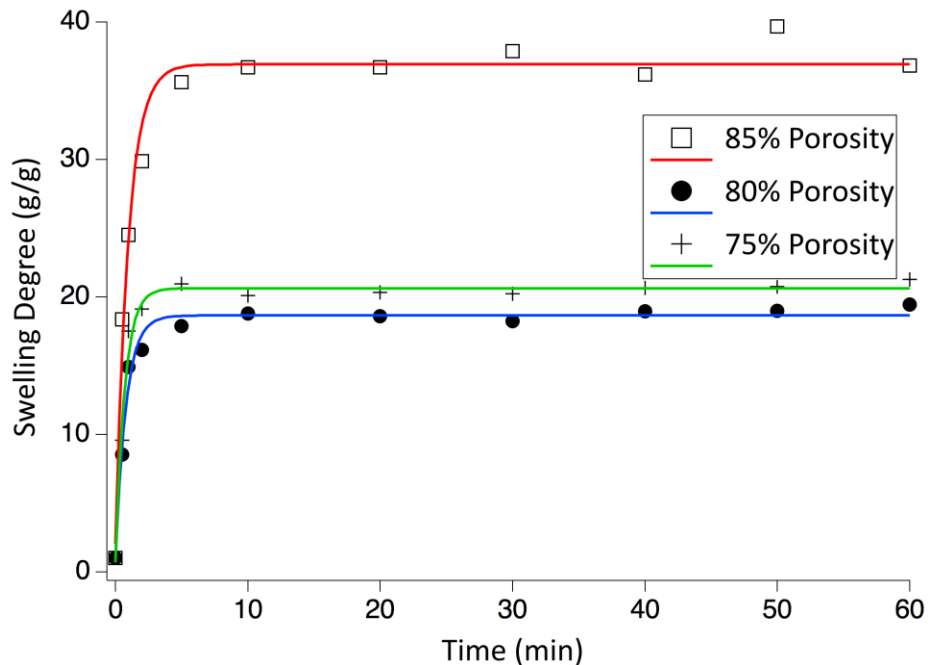


Figure 18: Water uptake ratio (grams of water/ grams of polyHIPE) of samples with different porosities

Transmission Electron Microscope

The in situ synthesized HFO nanoparticles were analyzed by transmission electron microscope (Figures 19 – 22). The synthesized HFO nanoparticles had two major morphologies: amorphous and cubic. The length of the nanoparticles particles was measured through image analysis using MATLAB software. Amorphous particles had a spindle shape so measuring their length was straightforward. The length and thickness of the amorphous nanoparticles showed an inverse relationship, which means the longer the particle the thinner it was. Two of the samples were studied under TEM: S_5_85 and S_4_85. These samples had 85% porosity and a monomer to cross-linker ratio of 5 to 1 and 4 to 1, respectively. The relation between monomer to crosslinking ratio and HFO nanoparticle size is that an increase in cross-linker content increases the rate of agglomeration of nanoparticles. The evidence of an increase in agglomeration is a decrease in amorphous particle size and increase in cubic particle size.

Table 1: Sizes of HFO nanoparticles within polyHIPE samples obtained from the TEM image analysis

	Average Amorphous Length	Average Cubic Length
S_5_85	113 ± 47 nm	20 ± 11 nm
S_4_85	89 ± 29 nm	33 ± 14 nm

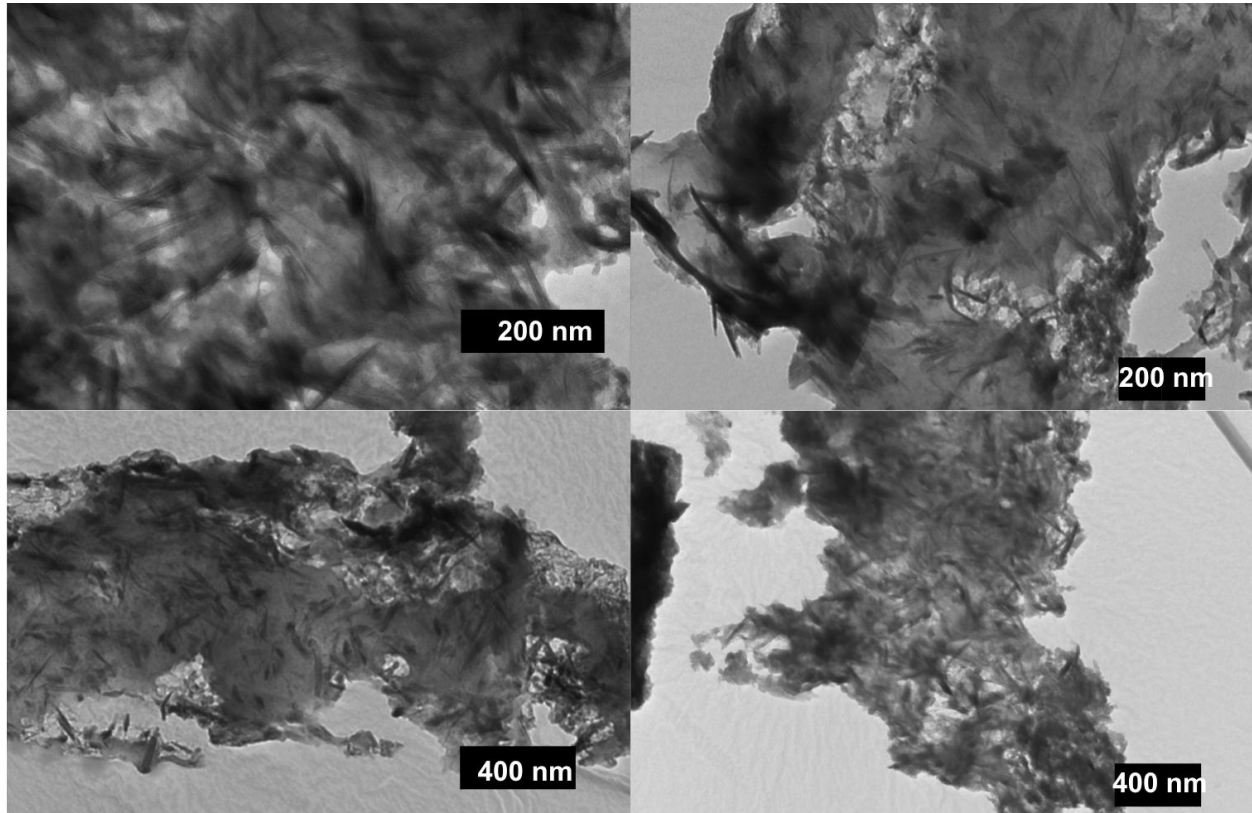


Figure 19: TEM micrographs of S_5_85 showing HFO nanoparticles with amorphous morphology. Magnification of the images to the top left 50,000x, top right 30,000x, bottom left 20,000x, and bottom right 15,000x.

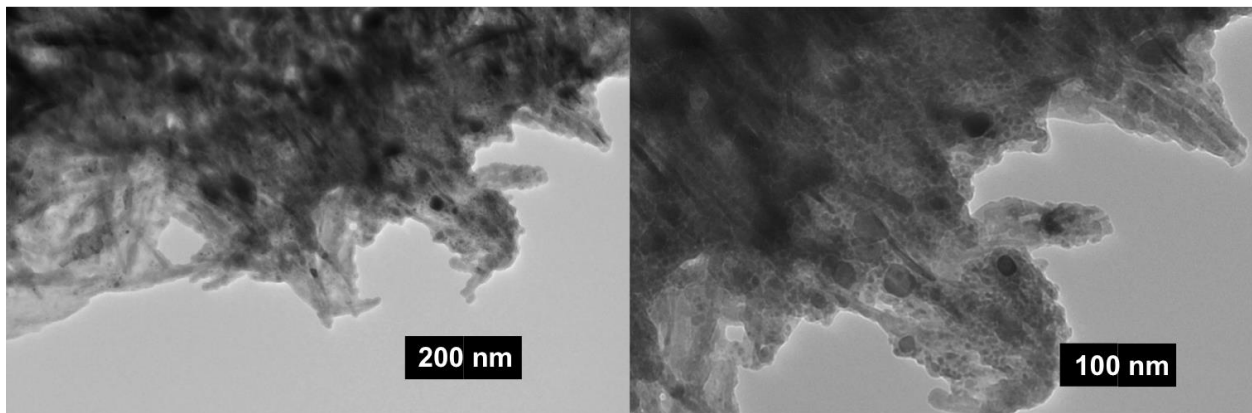


Figure 20: TEM micrographs of S_5_85 showing HFO nanoparticles with cubic morphology. Magnification of the images to the left is 40,000x and right 80,000x.

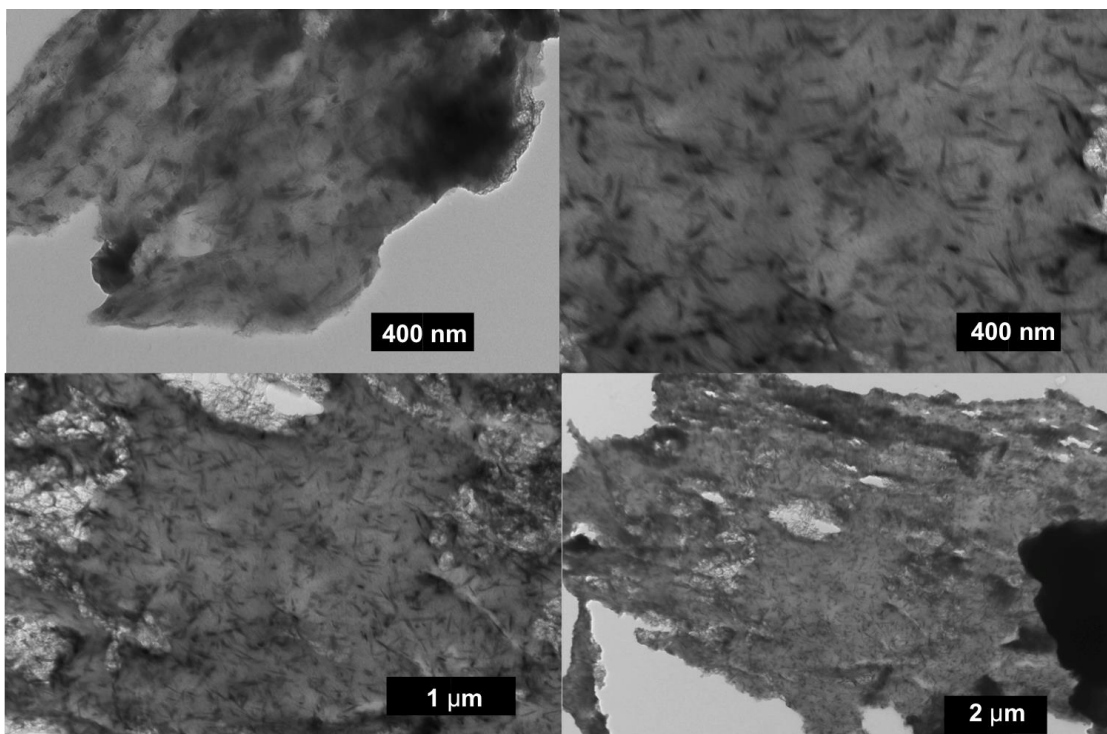


Figure 21: TEM micrographs of S_4_85 showing HFO nanoparticles with amorphous morphology. Magnification of the images to the top left 20,000x, top right 20,000x, bottom left 10,000x, and bottom right 4,000x.

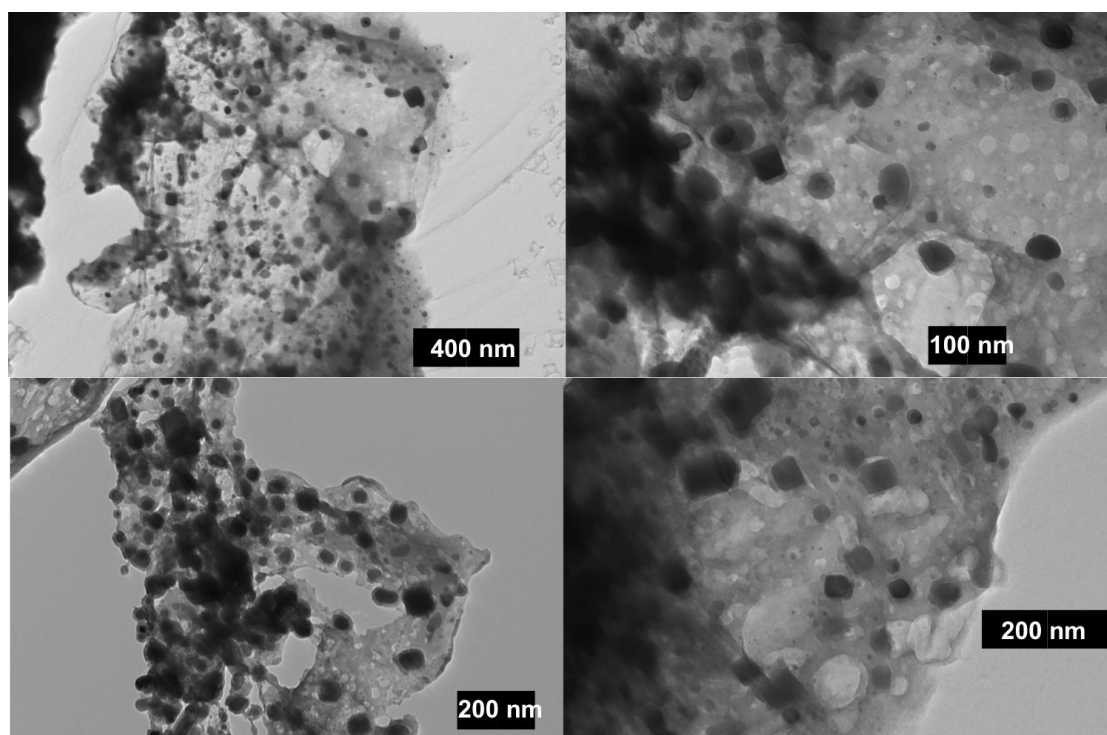


Figure 22: TEM micrographs of S_4_85 showing HFO nanoparticles with amorphous morphology. Magnification of the images to the top left 20,000x, top right 60,000x, bottom left 30,000x, and bottom right 50,000x.

Arsenic Removal

The samples were tested for their affinity to arsenic after HFO nanoparticles were incorporated in them. In most studies of arsenic removal, there is usually a packed bed column in which the water is directed through and the effluent is tested for arsenic contamination. Since this is a preliminary investigation of a new process, the method chosen is to simply place the samples in a plastic container filled with water having a concentration of 4.5 ppm As(V) for 24 hours. It should be noted that this concentration of arsenic is much higher than normally found in occurring water contamination, and further testing with lower concentrations (in the parts per billion range) must be tested for removal efficiency.

The results showed that the polyHIPE polymer functionalized with HFO particles can remove up to 60% of the As(V) ions in the solution. The arsenic removal compared functionalized and unfunctionalized polyHIPEs for different porosities and monomer to cross-linker ratio (Figure 24 and 24). Unfunctionalized polyHIPEs showed some removal of the arsenic cations, most likely because of the Donnan exclusion effect. In other words, the arsenic ions were able to enter the polyHIPE through the large pores, but became trapped by the overall charge of the sulfonic acid groups of polymerized AMPS (Cumbal and Sengupta 2005). There was an improvement of arsenic removal with the functionalization of the HFO particles once 85% porosity was reached (Figure 23). This most likely occurs because as the porosity increases the ease and efficiency of loading HFO nanoparticles into the polymer matrix increases due to improved diffusion from higher swelling and thinner matrix walls. The arsenic ions would also have an easier path moving through a polymer with higher porosity, which may be a factor in the removal percentage.

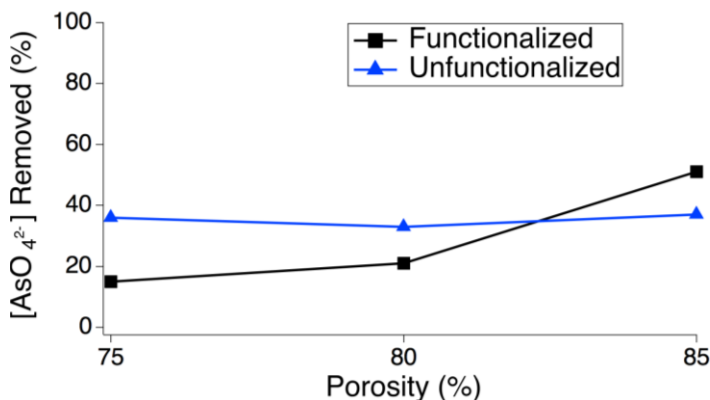


Figure 23: Percent of arsenic ions removed from solution for different porosities of functionalized and unfunctionalized polyHIPEs.

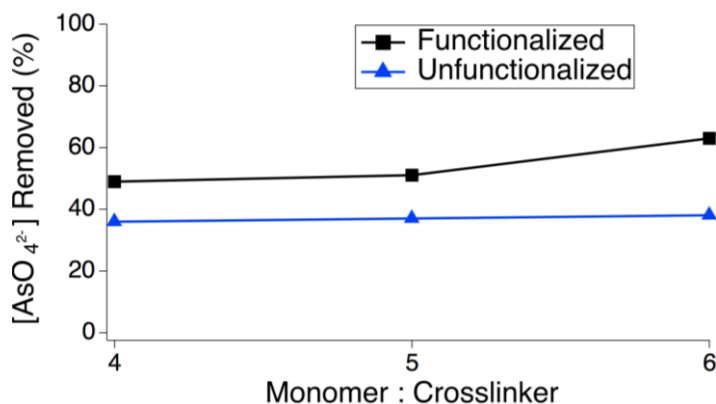


Figure 24: Percent of arsenic ions removed from solution for different monomer to cross-linker weight ratio of functionalized and unfunctionalized polyHIPEs.

Conclusion

Polymerized HIPEs of poly(2-acrylamido-2-methylpropanesulfonic acid) monoliths were successfully functionalized using an in-situ synthesis of hydrated ferric oxide (HFO) nanoparticles (analyzed through TEM), for the purpose of arsenic removal from water. The polyHIPE monoliths displayed extreme water uptake (~4000 wt.%, or ~40 gr water uptake per 1 gr of polymer) and hydrophilic capabilities due to their extensive porosity (analyzed through SEM), and charged surface from the sulfonic acid group. This finding paved the way for making next generation of supersorbent polymers for other water-related application. The functionalized polyHIPEs showed capabilities for removing up to 60% of arsenic from a 4.5 ppm concentration through adsorption, while the unfunctionalized polyHIPEs could also remove up to 35% of arsenic ions most likely through a Donnan Exclusion effect. It should be noted that 4.5 ppm concentration of arsenic is much higher than occurring level in water resources. In other words, we think that the incomplete removal was due to high arsenic level in water, and the produced polyHIPE could function more efficiently in low concentration of arsenic, which can be tested as a continuation of this work. Future work involving this method could also improve on the arsenic removal process by designing a setup with a flow method rather than batch method to ensure all of the water flows through the polyHIPE, and to accurately measure the lifetime of the polyHIPE in this process. Additionally, the supersorbent polyHIPEs discovered in this work can be used as hydrogels for variety of application in agriculture and biomedical industry.

Supporting Information

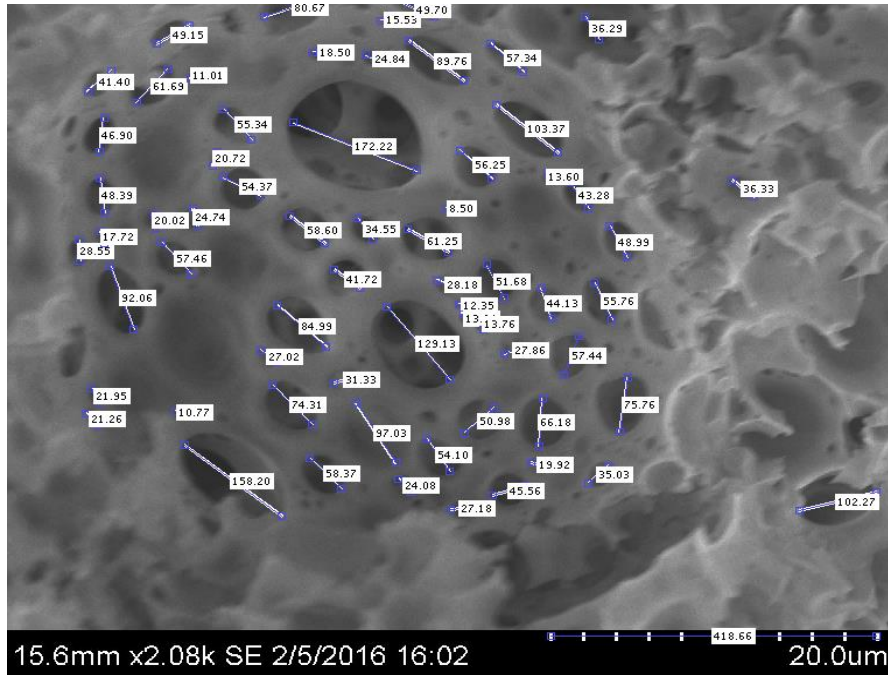


Figure 25: Typical image analysis of SEM micrographs in MATLAB measuring window diameter

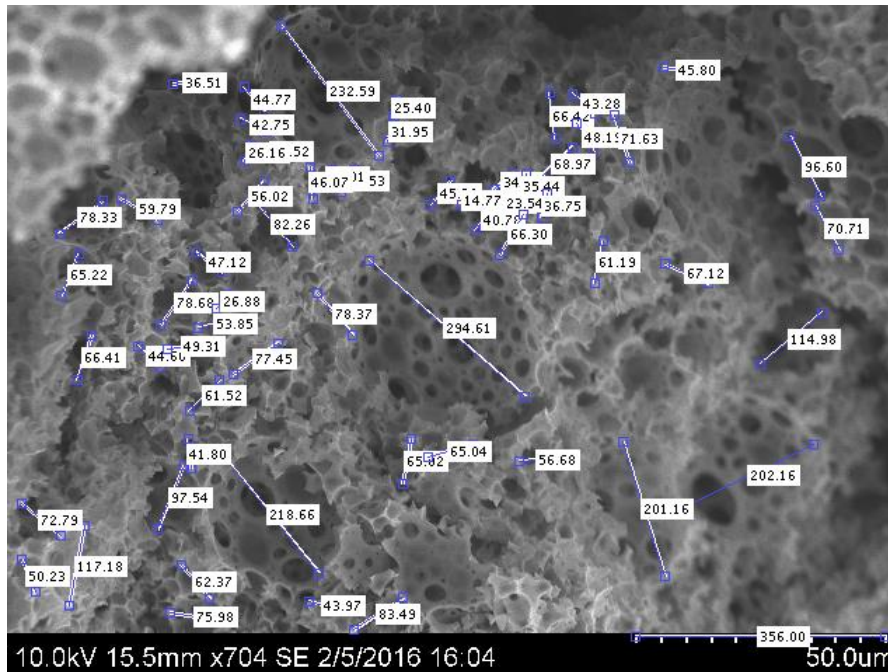


Figure 26: Typical image analysis of SEM micrographs in MATLAB measuring pore diameter

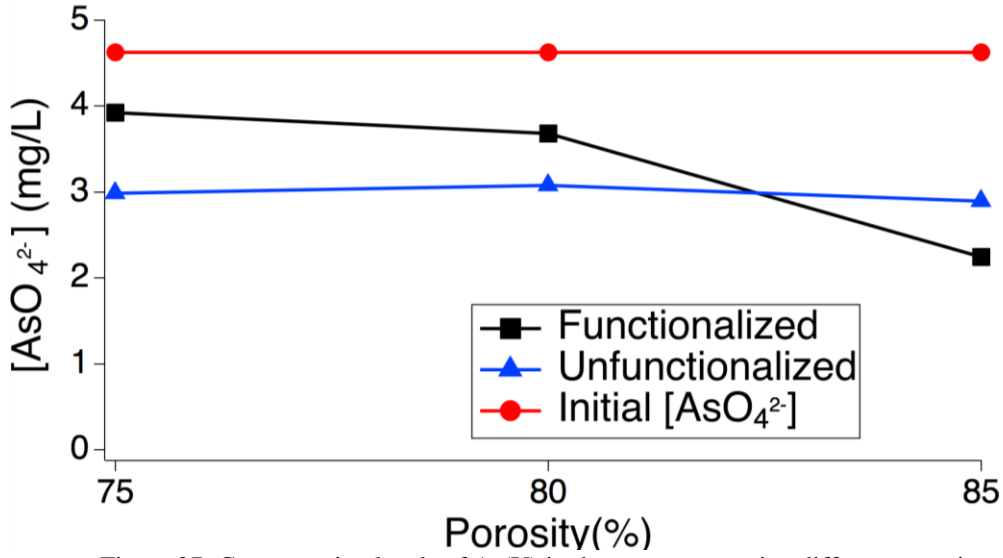


Figure 27: Concentration levels of As(V) in the water comparing different porosity of polyHIPEs

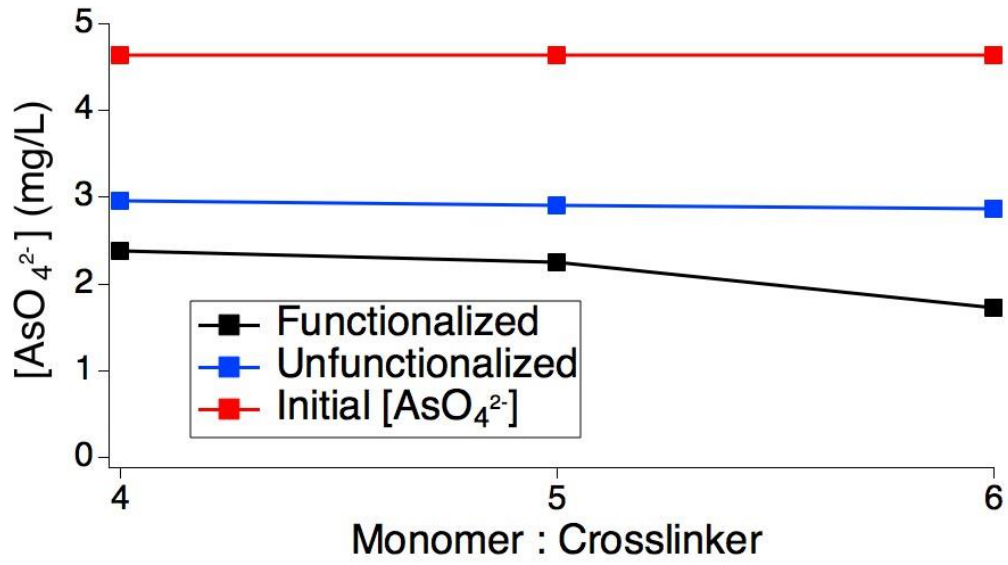


Figure 28: Concentration levels of As(V) in the water comparing different monomer to crosslinker weight ratios of polyHIPEs

References

- An, Byungryul, Qiqi Liang, and Dongye Zhao. "Removal of Arsenic(V) from Spent Ion Exchange Brine Using a New Class of Starch-bridged Magnetite Nanoparticles." *Water Research* 45, no. 5 (2011): 1961-972. doi:10.1016/j.watres.2011.01.004.
- Babak, Valery G., and Marie-José Stébé. "Highly Concentrated Emulsions: Physicochemical Principles of Formulation." *Journal of Dispersion Science and Technology* 23, no. 1-3 (2002): 1-22. doi:10.1080/01932690208984184.
- Baig, Shams Ali, Tiantian Sheng, Yunjun Hu, Jiang Xu, and Xinhua Xu. "Arsenic Removal from Natural Water Using Low Cost Granulated Adsorbents: A Review." *Clean Soil Air Water CLEAN - Soil, Air, Water* 43, no. 1 (2014): 13-26. doi:10.1002/clen.201200466.
- Boddu, Veera M., Krishnaiah Abburi, Jonathan L. Talbott, Edgar D. Smith, and Richard Haasch. "Removal of Arsenic (III) and Arsenic (V) from Aqueous Medium Using Chitosan-coated Biosorbent." *Water Research* 42, no. 3 (2008): 633-42. doi:10.1016/j.watres.2007.08.014.
- Cameron, Neil R. "High Internal Phase Emulsion Templating as a Route to Well-defined Porous Polymers." *Polymer* 46, no. 5 (2005): 1439-449. doi:10.1016/j.polymer.2004.11.097.
- Choong, Thomas S.y., T.g. Chuah, Y. Robiah, F.I. Gregory Koay, and I. Azni. "Arsenic Toxicity, Health Hazards and Removal Techniques from Water: An Overview." *Desalination* 217, no. 1-3 (2007): 139-66. doi:10.1016/j.desal.2007.01.015.
- Cumbal, Luis, and Arup K. Sengupta. "Arsenic Removal Using Polymer-Supported Hydrated Iron(III) Oxide Nanoparticles: Role of Donnan Membrane Effect †." *Environmental Science & Technology Environ. Sci. Technol.* 39, no. 17 (2005): 6508-515. doi:10.1021/es050175e.
- Dambies, Laurent. "Existing and Prospective Sorption Technologies for the Removal of Arsenic in Water." *Separation Science and Technology* 39, no. 3 (2005): 603-27. doi:10.1081/ss-120027997.
- Dimitrova, Tatiana D., and Fernando Leal-Calderon. "Rheological Properties of Highly Concentrated Protein-stabilized Emulsions." *Advances in Colloid and Interface Science* 108-109 (2004): 49-61. doi:10.1016/j.cis.2003.10.002.
- Fendorf, Scott, Peter S. Nico, Benjamin D. Kocar, Yoko Masue, and Katharine J. Tufano. "Arsenic Chemistry in Soils and Sediments." *Synchrotron-Based Techniques in Soils and Sediments Developments in Soil Science*, 2010, 357-78. doi:10.1016/s0166-2481(10)34012-8.
- Foudazi, Reza, Polina Gokun, Donald L. Feke, Stuart J. Rowan, and Ica Manas-Zloczower. "Chemorheology of Poly(high Internal Phase Emulsions)." *Macromolecules* 46, no. 13 (2013): 5393-396. doi:10.1021/ma401157b.
- Foudazi, Reza, Sahar Qavi, Irina Masalova, and Alexander Ya. Malkin. "Physical Chemistry of Highly Concentrated Emulsions." *Advances in Colloid and Interface Science* 220 (2015): 78-91. doi:10.1016/j.cis.2015.03.002.
- Fu, Fenglian, and Qi Wang. "Removal of Heavy Metal Ions from Wastewaters: A Review." *Journal of Environmental Management* 92, no. 3 (2011): 407-18. doi:10.1016/j.jenvman.2010.11.011.

- Gallegos-Garcia, Marisol, Kardia Ramírez-Muñiz, and Shaoxian Song. "Arsenic Removal from Water by Adsorption Using Iron Oxide Minerals as Adsorbents: A Review." *Mineral Processing and Extractive Metallurgy Review* 33, no. 5 (2012): 301-15. doi:10.1080/08827508.2011.584219.
- Ghorbani, Mohsen, and Hossein Eisazadeh. "Removal of COD, Color, Anions and Heavy Metals from Cotton Textile Wastewater by Using Polyaniline and Polypyrrole Nanocomposites Coated on Rice Husk Ash." *Composites Part B: Engineering* 45, no. 1 (2013): 1-7. doi:10.1016/j.compositesb.2012.09.035.
- Goddard, E.d. "Surfactants and Interfacial Phenomena." *Colloids and Surfaces* 40 (1989): 347. doi:10.1016/0166-6622(89)80030-7.
- Habuda-Stanić, Mirna, and Marija Nujić. "Arsenic Removal by Nanoparticles: A Review." *Environmental Science and Pollution Research Environ Sci Pollut Res* 22, no. 11 (2015): 8094-123. doi:10.1007/s11356-015-4307-z.
- Hassan, A.f., A.m. Abdel-Mohsen, and H. Elhadidy. "Adsorption of Arsenic by Activated Carbon, Calcium Alginate and Their Composite Beads." *International Journal of Biological Macromolecules* 68 (2014): 125-30. doi:10.1016/j.ijbiomac.2014.04.006.
- Höll, Wolfgang H. "Mechanisms of Arsenic Removal from Water." *Environ Geochem Health Environmental Geochemistry and Health* 32, no. 4 (2010): 287-90. doi:10.1007/s10653-010-9307-9.
- Jadhav, Sachin V., Eugenio Bringas, Ganapati D. Yadav, Virendra K. Rathod, Inmaculada Ortiz, and Kumudini V. Marathe. "Arsenic and Fluoride Contaminated Groundwaters: A Review of Current Technologies for Contaminants Removal." *Journal of Environmental Management* 162 (2015): 306-25. doi:10.1016/j.jenvman.2015.07.020.
- Kim, Eun-Sik, Yang Liu, and Mohamed Gamal El-Din. "The Effects of Pretreatment on Nanofiltration and Reverse Osmosis Membrane Filtration for Desalination of Oil Sands Process-affected Water." *Separation and Purification Technology* 81, no. 3 (2011): 418-28. doi:10.1016/j.seppur.2011.08.016.
- Lata, Sneha, and S.r. Samadder. "Removal of Arsenic from Water Using Nano Adsorbents and Challenges: A Review." *Journal of Environmental Management* 166 (2016): 387-406. doi:10.1016/j.jenvman.2015.10.039.
- Lim, Ai Phing, and Ahmad Zaharin Aris. "A Review on Economically Adsorbents on Heavy Metals Removal in Water and Wastewater." *Reviews in Environmental Science and Bio/Technology Rev Environ Sci Biotechnol* 13, no. 2 (2013): 163-81. doi:10.1007/s11157-013-9330-2.
- Lissant, K.j. "The Geometry of High-internal-phase-ratio Emulsions." *Journal of Colloid and Interface Science* 22, no. 5 (1966): 462-68. doi:10.1016/0021-9797(66)90091-9.
- Litter, Marta I., Maria E. Morgada, and Jochen Bundschuh. "Possible Treatments for Arsenic Removal in Latin American Waters for Human Consumption." *Environmental Pollution* 158, no. 5 (2010): 1105-118. doi:10.1016/j.envpol.2010.01.028.
- Lofrano, Giusy, Maurizio Carotenuto, Giovanni Libralato, Rute F. Domingos, Arjen Markus, Luciana Dini, Ravindra Kumar Gautam, Daniela Baldantoni, Marco Rossi, Sanjay K. Sharma, Mahesh Chandra Chattopadhyaya, Maurizio Giugni, and Sureyya Meric. "Polymer Functionalized Nanocomposites for Metals Removal from Water and Wastewater: An Overview." *Water Research* 92 (2016): 22-37.

doi:10.1016/j.watres.2016.01.033.

Masalova, Irina, Reza Foudazi, and A.ya. Malkin. "The Rheology of Highly Concentrated Emulsions Stabilized with Different Surfactants." *Colloids and Surfaces A: Physicochemical and Engineering Aspects* 375, no. 1-3 (2011): 76-86. doi:10.1016/j.colsurfa.2010.11.063.

Padungthon, Surapol, Michael German, Surases Wiriyathamcharoen, and Arup K. Sengupta. "Polymeric Anion Exchanger Supported Hydrated Zr(IV) Oxide Nanoparticles: A Reusable Hybrid Sorbent for Selective Trace Arsenic Removal." *Reactive and Functional Polymers* 93 (2015): 84-94. doi:10.1016/j.reactfunctpolym.2015.06.002.

Princen, H.m. "Highly Concentrated Emulsions. I. Cylindrical Systems." *Journal of Colloid and Interface Science* 71, no. 1 (1979): 55-66. doi:10.1016/0021-9797(79)90221-2.

Ramimoghadam, Donya, Samira Bagheri, and Sharifah Bee Abd Hamid. "ChemInform Abstract: Progress in Electrochemical Synthesis of Magnetic Iron Oxide Nanoparticles." *ChemInform* 45, no. 40 (2014). doi:10.1002/chin.201440223.

UN News Center. "The Human Right to Water and Sanitation Short Facts on the Human Right to Water and Sanitation Eight Short Facts on the Human Right to Water and Sanitation." November 2002. Accessed June 05, 2016. http://www.un.org/waterforlifedecade/human_right_to_water.shtml.

US EPA. Drinking Water Contaminants – Standards and Regulations. Accessed June 06, 2016. <http://water.epa.gov/drink/contaminants/basicinformation/arsenic.cfm>.

Zhang, Haifei, and Andrew I. Cooper. "Synthesis and Applications of Emulsion-templated Porous Materials." *Soft Matter* 1, no. 2 (2005): 107. doi:10.1039/b502551f.

Zhao, Xin, Lu Lv, Bingcai Pan, Weiming Zhang, Shujuan Zhang, and Quanxing Zhang. "Polymer-supported Nanocomposites for Environmental Application: A Review." *Chemical Engineering Journal* 170, no. 2-3 (2011): 381-94. doi:10.1016/j.cej.2011.02.071.